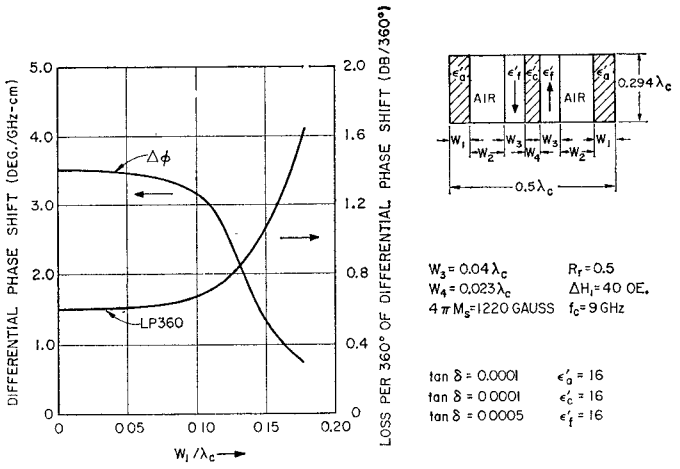

Fig. 4. Normalized loss and differential phase shift versus normalized slab width for slab against waveguide wall.

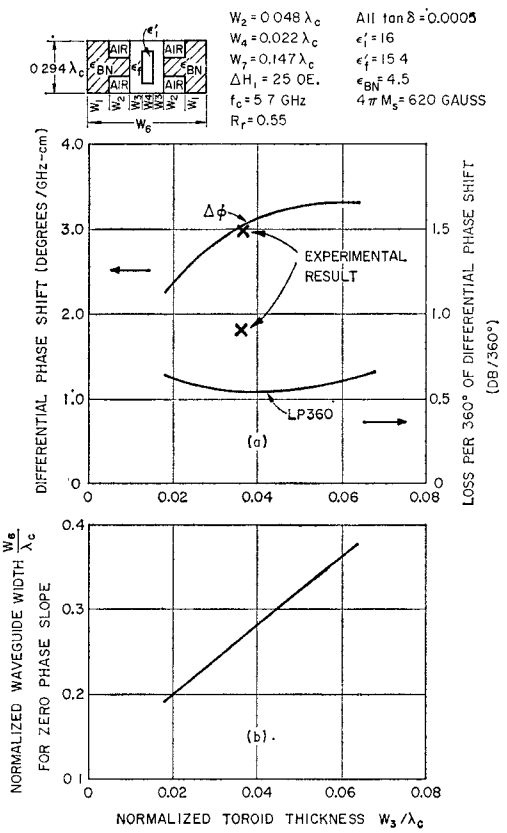

Fig. 5. (a) Normalized loss and differential phase shift versus normalized toroid wall thickness with constraint of zero phase slope. (b) Normalized waveguide width to produce zero phase slope for given value of toroid wall thickness.

can be seen from these curves, only a small sacrifice in phase shift and loss results from placing slabs of either of these materials against the toroid walls. The curve is included for reference and for $\epsilon_b' = 16$ shows a rapid decrease in differential phase shift with increasing cooling slab thickness. The results given in Fig. 4 show that placing dielectric slabs against the waveguide walls has little effect on phase shift or loss until the slabs are quite thick (e.g., about 0.1λ thick for $\epsilon_a' = 16$).

Characteristics of a phaser with T-shaped cooling sections of boron nitride are shown in Fig. 5. In the calculations, the W_2 region was replaced by an equivalent homogeneous slab with an effective dielectric constant calculated on a volume basis. Phasers are usually designed such that differential phase shift is independent of frequency over the operating band, i.e., the phase slope is zero. The curves of Fig. 5(a) incorporate this constraint. Differential phase shift and loss are shown as a function of toroid wall thickness with the constraint that the waveguide width is adjusted for each value of toroid wall thickness to produce zero phase slope at the center frequency. The waveguide width required for zero phase slope is given in Fig. 5(b). Structures of this type are quite effective in increasing the average power handling capability of ferrite latching phasers [4]. Differential phase shift and insertion loss for an experimental *C*-band phaser are shown for comparison. Note that the calculated data do not include waveguide copper losses.

Conclusion

An analysis has been presented of waveguide latching phaser structures useful for high average power applications. Calculated results show the effects on the loss and differential phase shift of adding vertical slab or T-shaped dielectric cooling structures. Design data presented permit a choice of toroid wall thickness and waveguide width to achieve optimum loss and phase characteristics with the constraint of zero phase slope.

References

[1] E. Schlomann, "Theoretical analysis of twin-slab phase shifters in rectangular waveguide," *IEEE Trans. Microwave Theory Tech.*, vol. MTT-14, pp. 15–23, Jan. 1966.
[2] W. J. Ince and E. Stern, "Computer analysis of ferrite digital phase shifters," in *IEEE Int. Conv. Rec.*, vol. 14, pt. 5, pp. 28–32, 1966.
[3] J. L. Allen, "The analysis of ferrite phase shifters including the effects of losses," Ph.D. dissertation, Georgia Inst. Technol., Atlanta, May 1966.
[4] G. P. Rodrigue, J. L. Allen, L. J. Lavedan, and D. R. Taft, "Operating dynamics and performance limitations of ferrite digital phase shifters," *IEEE Trans. Microwave Theory Tech. (1967 Symposium Issue)*, vol. MTT-15, pp. 709–713, Dec. 1967.
[5] Berger and Kapilevich, "Application of heat-removing ceramic dielectrics in SHF ferrite devices," *Radio Tekhnika*, vol. 25, pp. 79–83, 1971.
[6] H. Seidel, "Ferrite slabs in transverse electric mode waveguide," *J. Appl. Phys.*, vol. 28, Feb. 1957.

Low-Noise Microwave Down-Converter with Optimum Matching at Idle Frequencies

G. B. STRACCA, F. ASPESI, AND T. D'ARCANGELO

***Abstract*—A low-noise balanced down-converter for microwave radio-link applications is described. Down-converters of this type have been realized with typical noise figures of 3.5 dB at 4 GHz, 4 dB at 7 GHz, and 5 dB at 13 GHz. These results are obtained mainly by taking into account high order sideband frequencies of the pump harmonics up to the third, by properly terminating the image frequency, by matching the input port of the mixer and by optimizing the mixer–preamplifier interface. The experimental results are compared with the theoretical ones obtainable with ideal purely resistive diodes.**

I. Introduction

Theoretical analysis has shown that mixer performance depends not only on the RF/IF mixer impedances and on the image-frequency termination [1]–[4], but also on the terminations at the various "idle frequencies,"[1] as well as on the LO waveform [5]–[8].

This short paper describes a mixer configuration designed to control the idle-frequency terminations up to the third harmonic and gives experimental results for mixers operating at different frequency ranges (i.e., 3.6–4.2 GHz; 7.1–7.7 GHz; 12.7–13.3 GHz) which are now used in the receiving section of commercial radio links. Down-converters of the same type, operating at frequencies between 11 and 12 GHz, have also been developed for radiometric applications, and are presently in operation in various stations of the European Space Research Organization.

Manuscript received April 4, 1972; revised March 26, 1973.
G. B. Stracca is with the Istituto di Elettrotecnica ed Elettronica, Trieste University, Trieste, Italy.
F. Aspesi and T. D'Arcangelo are with the GTE Telecommunications Research Laboratories, Cassina de Pecchi, Milan, Italy.

[1] Idle frequencies are defined as follows: $\omega_{+m} = m\omega_p \pm \omega_0$, where ω_p is the LO frequency, ω_0 is the IF frequency, and m is any positive integer. Here, the frequency ω_{+1} is the signal frequency and ω_{-1} is the image frequency. When m is an even (odd) integer, the corresponding frequencies are called even (odd) "idle frequencies."

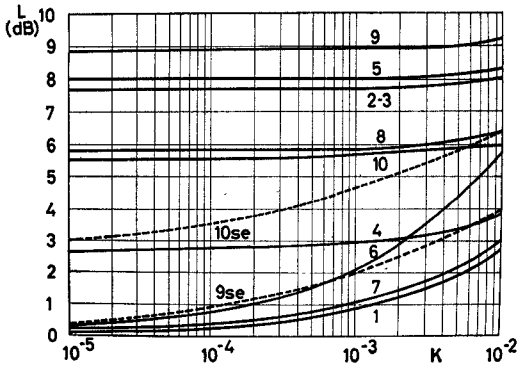

Fig. 1. Available conversion loss L_0 versus $k = g_{min}/g_{max}$ of resistive mixers. Solid lines—Balanced mixers with symmetrical rectangular LO drive waveform for the various cases of idle terminations given in Table I. Curve 9*se*—Single-ended mixer with optimum nonsymmetrical rectangular LO waveform (terminations as in case 9 of Table I). Curve 10*se*—Single-ended mixer with exponential resistive diode and sinusoidal voltage LO waveform (terminations as in case 10 of Table I).

TABLE I

IDLE-FREQUENCY TERMINATIONS FOR THE CASES OF FIG. 1

Cases	Odd Idle Frequencies		Even Idle Frequencies		
	ω_{-1}	all the others	ω_{-2}	ω_2	all the others
1	o.c.	o.c.	sh.c	sh.c	sh.c
2	sh.c	o.c.	sh.c	sh.c	sh.c
3	o.c.	o.c.	sh.c	o.c.	sh.c
4	o.c.	o.c.	o.c.	sh.c	sh.c
5	o.c.	o.c.	o.c.	o.c.	sh.c
6	sh.c	o.c.	sh.c	o.c.	sh.c
7	sh.c	o.c.	o.c.	sh.c	sh.c
8	sh.c	o.c.	o.c.	o.c.	sh.c
9	sh.c	sh.c	sh.c	sh.c	sh.c
10	o.c.	sh.c	sh.c	sh.c	sh.c

Note: Notice that the curves of Fig. 1 also hold for the dual termination cases, i.e., with short circuits (sh.c) replacing the corresponding open circuits (o.c.), and vice versa.

II. Design Considerations

1) Single-ended and balanced[2] mixer configurations have been analyzed with various LO drive waveforms and idle-frequency terminations with purely resistive diodes [5]–[7]. For both configurations, the best conversion losses are the same and are obtained with a symmetrical rectangular LO drive and with dual terminations at even and odd idle frequencies, respectively (i.e., with all the even idle frequencies short circuited and all the odd idle frequencies open circuited, or vice versa).

In order to compare the best theoretical performance with the experimental results, the theoretical conversion loss L_0 calculated for input and output conjugate match conditions (i.e., "available" conversion loss) is plotted in curve 1 of Fig. 1 versus $k = g_{min}/g_{max}$, where g_{min} and g_{max} are the minimum forward and the maximum reverse differential diode conductance during the pump cycle, respectively.

This type of idle-frequency termination can easily be realized in balanced mixers, because all the odd idle frequencies appear at the input and all the even appear at the output,[2] which allows the corresponding constraints to be set, at least in theory, by means of two filters only at the input and output port, respectively.

Single-ended mixers do not present even and odd idle-frequency separations, and therefore an infinite number of filters is necessary to set the optimum terminations. Single-ended mixers, however, have been analyzed until now by imposing the same kind of constraints at all the idle frequencies (i.e., short circuit or open circuit), and only at a finite number of frequencies (ω_{-1} [1], [4], [6]; ω_2; and ω_{-2} [5], [7]) has the influence of different terminations been examined. In this case, in fact, the imbedding network may again be realized with a small number of filters. Suboptimal operating conditions have been found, which require nonsymmetrical rectangular LO waveforms and the same kind of terminations for all the idle frequencies [4], [5].[3] The curve 9*se* of Fig. 1 shows the behavior of L_0 in this case.

The balanced mixer configuration has finally been selected for the practical design described in Section III, because of the intrinsic simplicity in setting the optimum idle-frequency constraints as discussed above.

2) It is difficult to drive the diodes at microwave frequencies with a rectangular waveform. For the case of a sinusoidal waveform, theoretical analysis indicates that a sinusoidal current is better than a sinusoidal voltage [6], [7]. As an example, for $k = 10^{-3}$, the degradation of L_0 is about 1 dB for a sinusoidal LO current and 3 dB for a sinusoidal LO voltage with respect to curve 1 of Fig. 1. In the actual mixer, therefore, the LO signal is coupled to the diodes through a series resonator, which presents high impedance to LO harmonic frequencies and allows us to approximate better a sinusoidal current drive than a sinusoidal voltage drive.

3) In practical cases, mixer diodes are not purely resistive. However, measured results show good agreement with theory, provided the k value, chosen to characterize the diodes, is defined as the ratio of the minimum to the maximum real part of the diode small-signal admittance at the LO frequency, measured at 0 V and at full conduction bias conditions, respectively.

4) To show the influence of different idle-frequency terminations, we have also plotted in Fig. 1 L_0 versus k for the various cases defined in Table I, still for the same LO waveform. Notice that the dual cases are equivalent as far as conversion losses are concerned. However, they may exhibit different noise figures, as discussed in [7].

The behavior of L_0 at small k's for cases 2–5 and 8–10 can be justified heuristically by observing that some components of the currents circulating in the resistive diodes become very large as k approaches zero, in order to satisfy the constraints imposed at the input and output ports. It may be noticed that the idle-frequency terminations of cases 9 and 10 for balanced mixers are the same as those of the suboptimal cases for single-ended mixers mentioned before, and are presented in curves 9*se* and 10*se*.

Experiments have confirmed the influence of idle-frequency terminations in practical mixers with real diodes and nonrectangular LO waveforms, but the differences are not so pronounced, as shown in the theoretical cases of Fig. 1.

5) It is well known [3], [7] that the source impedance, which gives the minimum conversion loss, is not generally coincident with that giving the minimum down-converter noise figure. However, in practical situations, there is little difference in noise performance between the two cases [7], and therefore the mixer has been adjusted for a source impedance corresponding to that of minimum conversion loss.

6) To minimize the overall noise figure, particular care should be given to the mixer/IF preamplifier interface. For minimum noise, an impedance transformer should be used to transform the mixer output impedance into the optimum IF source impedance. To avoid the difficulties associated with the realization of a transformer network, an IF preamplifier has been realized which has an optimum noise source impedance close to the output impedance of the mixer.

III. Description of the Experimental Mixer

A schematic representation of the experimental balanced two-diode mixer is shown in Fig. 2. The mixer consists of a waveguide cavity containing an alumina substrate with two beam lead Schottky-barrier diodes mounted thereon.

The mixer configuration is designed to control the idle-frequency terminations up to the third harmonic. The image frequency ω_{-1} is terminated by properly positioning an image rejection filter at the input. This filter consists of two capacitively coupled bandstop coaxial resonators which are spaced a quarter wavelength at the band-

[2] The term "balanced" refers both to the four-diode configuration discussed in [9] and to the equivalent two-diode configuration of Fig. 2, i.e., for configurations in which there exist inherent even and odd idle-frequency isolations (and therefore inherent-signal IF isolation). Hybrid coupled two-diode mixers (although often called balanced mixers) do not present this property, and are considered as single-ended mixers.

[3] When a sinusoidal voltage LO waveform is applied to a diode with an ideal exponential V–I characteristic and all the idle frequencies higher than ω_{-1} are short-circuited, the optimum operation is achieved when ω_{-1} is open circuited (see curve 10*se* of Fig. 1).

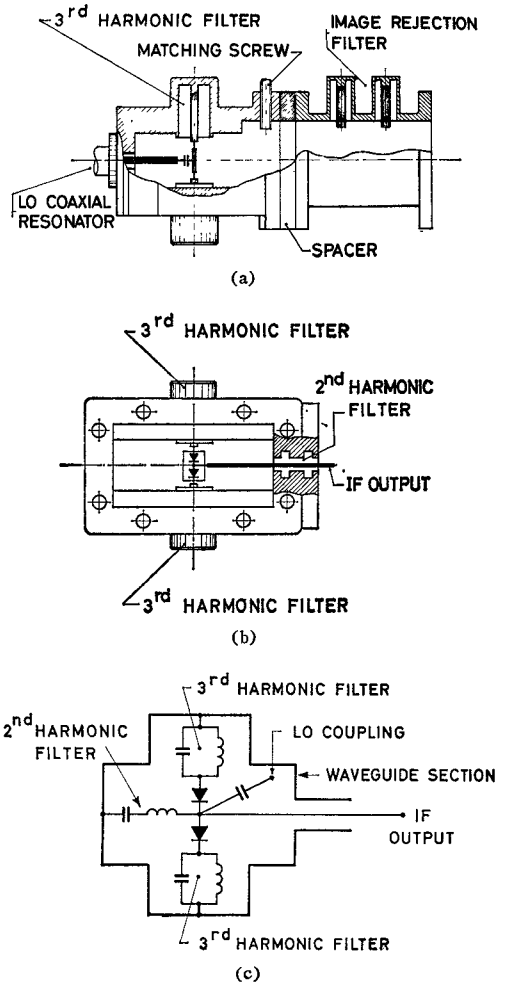

Fig. 2. (a) Mixer longitudinal cross-section view. (b) Mixer transverse cross-section view. (c) Mixer equivalent circuit.

stop center frequency. It can be tuned over a band of about 700 MHz and exhibits the following characteristics:

power reflected in the image frequency band (25 MHz) ≥ 80 percent;

insertion loss in the signal frequency band (25 MHz) ≤ 0.1 dB.

The electrical distance between the image rejection filter and the diodes' plane determines the actual admittance seen by the diodes at the image frequency, and is chosen to provide an open circuit at the diodes' plane. The distance can be varied by means of suitable spacers placed between the mixer cavity and the image rejection filter.

The currents at the third-harmonic idle frequencies $\omega_{\pm 3}$ are open circuited by means of fixed-tuned coaxial resonators connected to the diodes. The second-harmonic idle frequencies $\omega_{\pm 2}$ are properly short circuited at the output port by means of a suitable series resonator at the IF output port.[4]

The LO signal is capacitively coupled to the diodes from the rear of the waveguide. This type of coupling allows the use of a series resonator for achieving a sinusoidal current waveform.

To match the mixer-input impedance to the standard waveguide, the diodes are mounted in a reduced-height waveguide section.

The two diodes, which are in parallel at the mixer output, are connected directly to the IF-preamplifier input. The first stage of the IF preamplifier consists of a low-noise transistor in the common-emitter configuration. The transistor has been selected for an optimum noise source impedance approximately equal to the output impedance of the mixer when it is adjusted for minimum conversion loss. Fig. 3 shows the noise figure of different low-noise transistors as a function of the source impedance. The collector current level to which the curves of Fig. 3 refer has been chosen as a compromise to meet the intermodulation requirements of the overall receiving system due to the presence of adjacent channels and to minimize the IF noise figure.

[4] A double-balanced four-diode mixer has also been tested, which uses an interdigitated capacitor to short circuit all the even idle frequencies at the output port of the mixer [10]. However, the two-diode balanced mixer configuration previously described has finally been selected because it allows a simpler implementation of the mixer–IF interface with no appreciable degradation of the conversion losses.

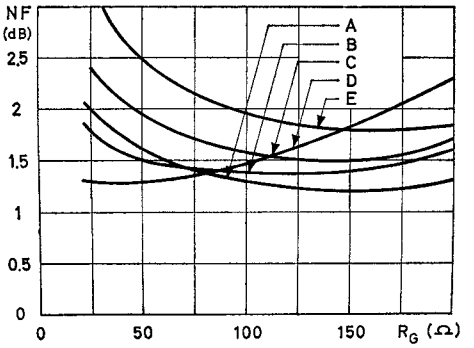

Fig. 3. Source impedance–dependence of IF preamplifier noise figure for various first-stage transistors. *A*—Texas Instruments MS 175 H; *B*—Avantek AT17A; *C*—Texas Instruments MS 173 H; *D*—KMC K6001; *E*—NEC V871.

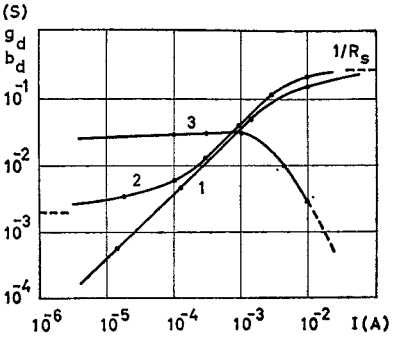

Fig. 4. Typical measured mixer diode dc and RF differential admittances as functions of diode dc current. 1—Differential dc conductance; 2—differential conductance at 7.350 GHz; 3—differential susceptance at 7.350 GHz.

Fig. 3 shows that the use of transistor *A* optimizes the IF noise figure with an output mixer impedance of about 125 Ω. This value of the output impedance is practically the same for all the Schottky-barrier diode types which have been tested.

The diode types are 1) the HP 5082-2709 for mixers operating in the 4- and 7-GHz ranges; and 2) the AEI DC 1306 for mixers operating in the 13-GHz range.

To show the difference between a practical nonlinear device and the ideal resistive diode, which the curves of Fig. 1 refer to, both the dc and RF admittances of the HP 5082-2709 diode are shown in Fig. 4. The results are plotted as a function of the diode current; curve 1 shows the differential dc conductance; curve 2 shows the differential conductance measured at 7350 MHz; and curve 3 shows the differential susceptance. Notice that the dc forward characteristic follows that of an exponential diode (i.e., $g = g_0 e^{-V/V_D}$, with $V_D = 31$ mV instead of the theoretical 25 mV) in series with a resistor R_S (with $R_S = 3.8$ Ω). The dc differential conductance approaches the limiting value $1/R_S$ for large currents ($I > 2$ mA). For reverse currents, the dc differential conductance does not decrease following the exponential law, but exhibits a minimum value of 10^{-7} Ω^{-1} at $I = -0.7$ μA. The diagram shows that at microwave frequencies, because of the presence of the diode junction capacity, the ratio g_{min}/g_{max} is markedly higher than the corresponding dc ratio ($3.8 \cdot 10^{-7}$). At 7350 MHz, for example, the ratio has been measured to be $5 \cdot 10^{-3}$.

It may be interesting to notice that, even though the curves in Fig. 1 refer to an idealized situation (purely resistive diodes and symmetrical rectangular LO waveform drive), the measured conversion losses are very close to the values given by the theoretical curve of case 1, when a k value is assumed equal to the ratio g_{min}/g_{max} measured at the appropriate microwave frequency.

As a typical example of practical realizations, Fig. 5 shows the 4-GHz version of the complete down-converter.

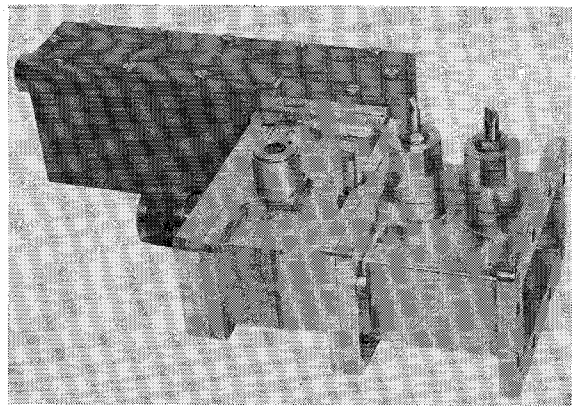

Fig. 5. Low-noise 4-GHz down-converter.

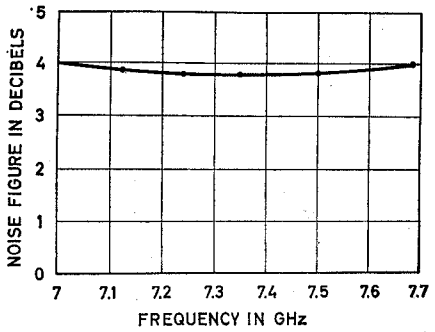

Fig. 6. Measured noise figure response of representative down-converter.

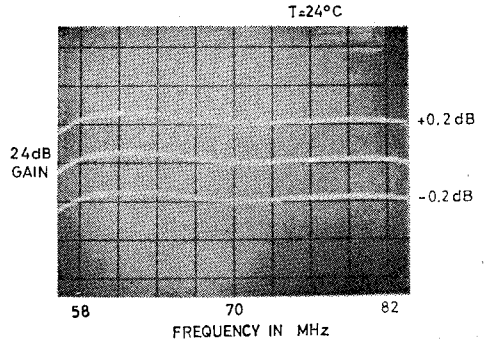

Fig. 7. Representative down-converter instantaneous overall gain-frequency response.

TABLE II

SUMMARY OF MEASURED PERFORMANCE OF RADIO-LINK MIXERS

RF input-signal tuning range	3.6–4.2 GHz	7.1–7.7 GHz	12.7–13.3 GHz
Overall noise figure at ambient temperature (including losses of image reject filter)	3.2 dB min 3.5 dB max	3.7 dB min 4 dB max	5 dB min 5.3 dB max
IF noise figure	1.5 dB	1.5 dB	1.5 dB
Conversion loss	2 dB max	2.6 dB max	4 dB max
Intermediate frequency		70 MHz	
Overall down-conversion gain of the receiver		24 dB	
Frequency response over any 25-MHz band	flat ±0.05 dB at ambient temperature ±0.2 dB from −5°C–55°C ±0.2 dB with ±2-dB pump power variation		
Diodes employed	HP 5082–2709	HP 5082–2709	AEI DC 1306
Rectified current	1 mA	1 mA	2 mA
AM/PM conversion	0.2°/dB at an input RF level of −20 dBm		

IV. Experimental Results

Down-converters in the configuration described in Section III have been realized in the whole frequency range from 4 to 13 GHz. The measured performance of three down-converter versions, designed for microwave radio-link equipment, operating in the frequency ranges of 3.6–4.2 GHz, 7.1–7.7 GHz, and 12.7–13.3 GHz, respectively, are summarized in Table II.

The RF tunable range, indicated in Table II, is covered by mechanically retuning the image rejection filter only. No tuning is needed for both the second-harmonic and third-harmonic idle-frequency filters. It has been found experimentally that the position of the image rejection filter is not critical. Only two electrical distances (i.e., only one spacer) are sufficient to cover the entire RF input-signal tuning range.

Typical behavior of the noise figure of a down-converter unit within the RF frequency range is shown in Fig. 6. In addition to the results given in Table II, a typical example of an instantaneous gain-frequency response is shown in Fig. 7; such a response is practically the same in the whole RF frequency range.

References

[1] H. C. Torrey and C. A. Whitmer, *Crystal Rectifiers* (M.I.T. Radiation Laboratory Series), vol. 15. New York: McGraw-Hill, 1948.
[2] P. D. Strum, "Some aspects of crystal mixer performance," *Proc. IRE*, vol. 41, pp. 875–889, July 1953.
[3] R. J. Mohr and S. Okwit, "A note on the optimum source conductance of crystal mixers," *IRE Trans. Microwave Theory Tech.*, vol. MTT-8, pp. 622–627, Nov. 1960.
[4] M. R. Barber, "Noise figure and conversion loss of the Schottky barrier mixer diode," *IEEE Trans. Microwave Theory Tech.*, vol. MTT-15, pp. 629–635, Nov. 1967.
[5] G. B. Stracca, "On frequency converters using non-linear resistors," *Alta Freq.*, vol. 38, pp. 318–331, May 1969.
[6] A. A. M. Saleh, *Theory of Resistive Mixer*. Boston, Mass.: M.I.T. Press, 1971.
[7] G. B. Stracca, "Noise in frequency mixers using non-linear resistors," *Alta Freq.*, vol. XL, no. 6, pp. 484–505, 1971.
[8] F. Aspesi and T. D'Arcangelo, "Low-noise down converter for radio link application," presented at the 1971 European Microwave Conf., Stockholm, Sweden.
[9] R. S. Caruthers, "Copper oxide modulators in carrier telephone systems," *Bell Syst. Tech. J.*, vol. XVIII, pp. 305–337, Apr. 1939.
[10] G. B. Stracca and C. Bassi, "Balanced and unbalanced frequency converters using non-linear resistor," presented at the Microwave Colloq., Budapest, Hungary, Apr. 1970.

Matching Considerations of Lossless Reciprocal 5-Port Waveguide Junctions

A. L. HIEBER AND R. J. VERNON

***Abstract*—Some of the restrictions imposed on general 5-port junctions (or networks) by losslessness and reciprocity are discussed as well as considerations of restrictions due to physical symmetry. It is proven that if a lossless reciprocal 5-port junction (or network) is completely matched, then all off-diagonal elements of the scattering matrix are nonzero; i.e., if the junction is matched, no port is decoupled from any of the others. It is also shown that all off-diagonal scattering coefficients of a lossless reciprocal 5-port junction (or network) have a magnitude of one half if and only if the junction is completely matched. Those physical symmetries which preclude complete matching of 5-port junctions are given and a general theorem concerning the matching of junctions and physical symmetry is proven.**

I. Introduction

It has long been established that lossless reciprocal waveguide junctions[1] having three or four electrical ports exhibit certain properties pertaining to complete matching and port decoupling, which may be determined from the fact that the scattering matrix of such a junction must be both unitary and symmetric [1], [6]. In addition

Manuscript received July 7, 1972; revised January 8, 1973. This work was supported by the National Science Foundation through a traineeship for A. L. Hieber.

A. L. Hieber was with the Department of Electrical Engineering, University of Wisconsin, Madison, Wis. 53706. He is now with Missile Systems Division, Raytheon Company, Bedford, Mass. 01730.
R. J. Vernon is with the Department of Electrical Engineering, University of Wisconsin, Madison, Wis. 53706.

[1] The more general term "network" may be used throughout this short paper in place of the terms "waveguide junction" except where the physical symmetry of the junction is specified.